experimental evidence, including a direct demonstration with electron paramagnetic resonance spectroscopy (*9*), has shown the presence of a substantial quantity of the O_2^- ion in this system. By analogy, it is expected that singlet molecular oxygen would be generated in this enzymatic system, and this expectation is strongly supported by the observed chemiluminescence of a number of organic molecules present in the xanthine oxidase system (*10*). Since a large number of biological oxidative processes are thought to proceed by way of an "electron transfer" step, the possibility of the involvement of singlet oxygen in such systems needs careful evaluation.

The reaction of potassium superoxide with water is the single most important *chemical* source of oxygen for breathing purposes in hospitals (*11*), mines, submarines (*12*), and space capsules (*13*). Even if only a small fraction of singlet oxygen survives quenching, it could prove to be a serious health hazard.

AHSAN U. KHAN
Institute of Molecular Biophysics, Florida State University, Tallahassee 32306

References and Notes

1. A. U. Khan and M. Kasha, *J. Chem. Phys.* **39**, 2105 (1963); *Nature* **204**, 241 (1964); *J. Amer. Chem. Soc.*, in press; M. Kasha and A. U. Khan, *Ann. N.Y. Acad Sci.*, in press; S. J. Arnold, E. A. Ogryzlo, H. Witzke, *J. Chem. Phys.* **40**, 1769 (1964); R. J. Browne and E. A. Ogryzlo, *Proc. Chem. Soc. London* **1964**, 117 (1964); J. S. Arnold, R. J. Browne, E. A. Ogryzlo, *Photochem. Photobiol.* **4**, 963 (1965).
2. A. U. Khan and M. Kasha, *J. Amer. Chem. Soc.* **88**, 1574 (1966).
3. C. S. Foote, *Accounts Chem. Res.* **1**, 104 (1968).
4. C. S. Foote, M. T. Wuesthoff, S. Wexler, I. G. Burstain, R. Denney, G. O. Schenck, K. H. Schulte-Elte, *Tetrahedron* **23**, 2583 (1967).
5. L. W. Bader and E. A. Ogryzlo, *Discuss. Faraday Soc.* **37**, 46 (1964).
6. K. D. Legg and D. M. Hercules, *J. Amer. Chem. Soc.* **91**, 1902 (1969).
7. F. McCapra and R. A. Hann, *Chem. Commun.* **1969**, 443 (1969).
8. I. Fridovich and P. Handler, *J. Biol. Chem.* **233**, 1578 (1958); *ibid.*, p. 1581; *ibid.* **236**, 1836 (1961); *ibid.* **237**, 916 (1962).
9. V. Massey, S. Strickland, S. G. Mayhew, L. G. Howell, P. C. Engel, R. G. Matthews, M. Schuman, P. A. Sullivan, *Biochem. Biophys. Res. Commun.* **36**, 891 (1969); D. Ballou, G. Palmer, V. Massey, *ibid.*, p. 898; W. H. Orme-Johnson and H. Beinert, *ibid.*, p. 905.
10. J. R. Totter, E. C. de Dugros, C. Riveiro, *J. Biol. Chem.* **235**, 1839 (1960).
11. W. A. Noyes, Jr., Ed., *Science in World War II: U.S. Office of Scientific Research and Development, Chemistry* (Little, Brown, Boston, 1948), vol. 6, p. 363.
12. J. Clarke, *J. Amer. Chem. Soc. Nav. Eng.* **68**, 105 (1956).
13. R. M. Bovard, *Aerospace Med.* **31**, 407 (1960).
14. Supported by a contract between the Division of Biology and Medicine, U.S. Atomic Energy Commission, and Florida State University. I thank Professor M. Kasha for his suggestions and encouragement, Dr. M. G. Nair for his help with the chemical scavenger experiment, and Dr. R. Light for bringing to my attention the biological references.

24 November 1969

Lunar Gravity over Large Craters from Apollo 12 Tracking Data

Abstract. *The Doppler residuals from the Apollo 12 lunar module radio tracking data indicate large negative accelerations over the craters Ptolemaeus and Albategnius. The mass deficiencies required to produce these accelerations are approximately equivalent to the removal of the surface material to a depth of 1 kilometer over the entire area of these craters. Several other features of the gravity fine structure can also be correlated with topography.*

The ballistic portion of the descent trajectory of the Apollo 12 lunar module presented a unique opportunity to observe strong accelerations due to lunar surface gravity fine structure (less than 5° in diameter). Previous Doppler radio tracking S-band data from the five Lunar Orbiters have permitted estimation of accelerations caused by surface features greater than 10° (300 km) in diameter (*1–3*). Since most of the Lunar Orbiter data were obtained above an altitude of 100 km, the very fine structural features, such as craters, were unresolved. The ballistic portion of the lunar module descent trajectory approached to within 12 km of the lunar surface, and this close approach therefore makes possible the resolution of accelerations caused by features 50 km in diameter.

Unfortunately, the Apollo 10 and 11

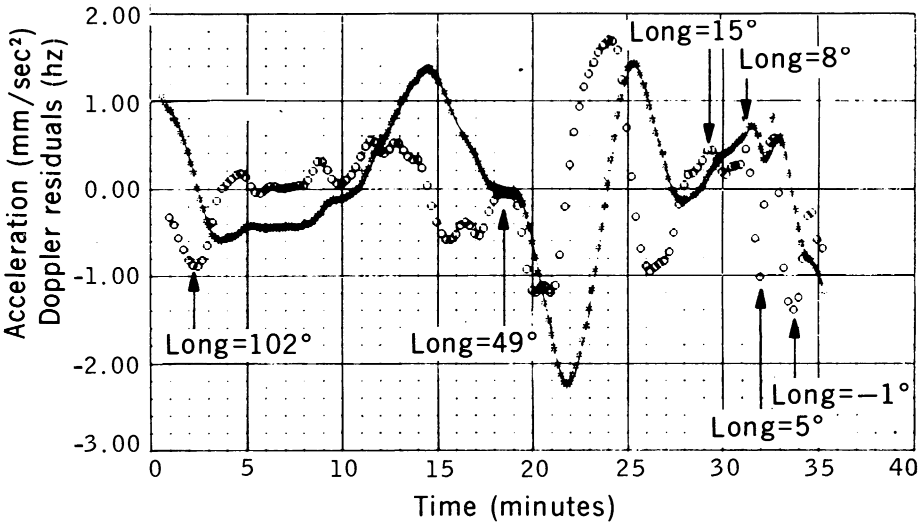

Fig. 1. Earthward velocity residuals (asterisks), and resulting accelerations (circles), after a triaxial model orbit determination.

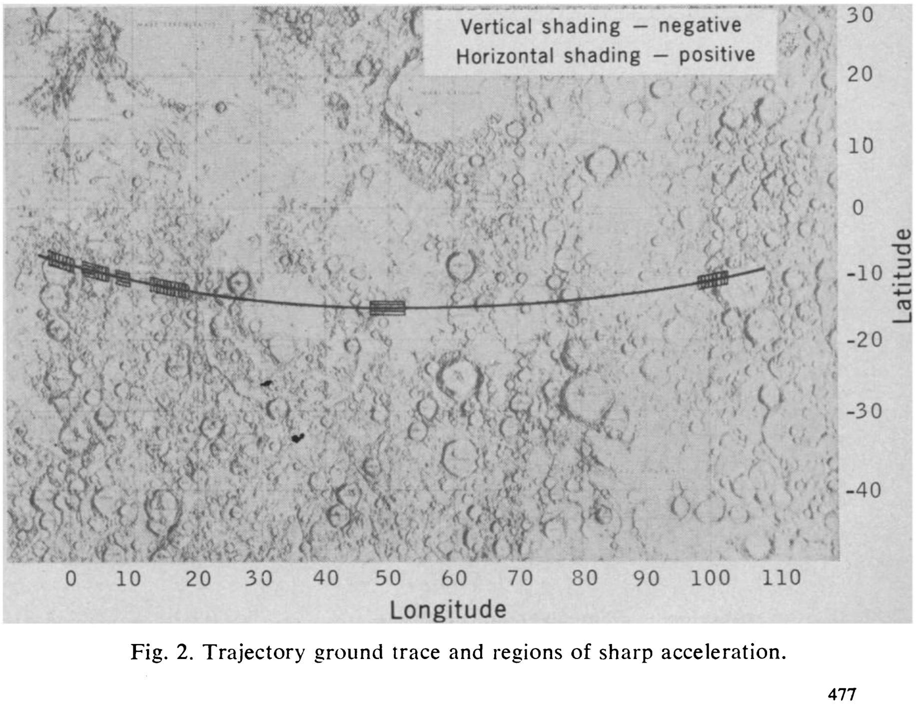

Fig. 2. Trajectory ground trace and regions of sharp acceleration.

Table 1. Mass deficiencies at detected locations.

Crater	Acceleration after		Spacecraft altitude (km)	Equivalent crater depth (km)
	Triaxial fit (mgal)	20th order fit (mgal)		
Ptolemaeus	−140	−87	14	1.0
Albategnius	−100	−88	15	1.2
Unnamed crater (latitude −12°, longitude 105°)	− 90	−60	76	2.1

descent phases were subject to communication losses which left such large gaps in the Doppler tracking data that it was impossible to obtain meaningful information on gravity fine structure (*4*). The Apollo 12 lunar module, however, was tracked successfully during the entire 30-minute portion of the descent trajectory visible from the earth. The Doppler measurements were taken at 10-second and 1-second intervals. The spacecraft initial state was estimated on the basis of these line-of-sight velocity measurements with a simple triaxial model for trajectory integration. The remaining velocity residuals were differentiated to provide a least-squares filtered estimate of the accelerations due to the fine structure of the near-surface lunar gravity field, as was done for Lunar Orbiter data (*1*). Simulation studies (*3, 5*) have shown that this procedure provides precise location of near-surface gravity anomalies, with estimates of the magnitude of the actual accelerations accurate to within 30 percent.

The Doppler residuals of the data measured at 10-second intervals, obtained by the above procedure, are shown in Fig. 1. The accelerations obtained by differentiating a sequence of patched cubic polynomials fitted to these residuals are also shown. The largest positive acceleration occurs over the Mare Nectaris, already known to be the location of a mascon (*1*). The locations of the other sharp accelerations are shown in Fig. 2, superimposed on a ground trace of the descent trajectory. The data measured at 1-second intervals show the same features.

In order to reduce the spurious effects caused by the mascon at Mare Nectaris, the data were also fitted with a 20th degree and order spherical harmonic gravity model (*3*), which was constructed to fit the Doppler velocities from Lunar Orbiter tracking data. The resulting residuals and accelerations are shown in Fig. 3. Over the region of interest, this model has significant gravity anomalies at Mare Smythii and Mare Nectaris and, as would be expected, the residuals in these regions are substantially reduced by comparison with residuals obtained with the triaxial model (Fig. 1). More importantly, the spurious large residuals at the ends of the data span have also been eliminated.

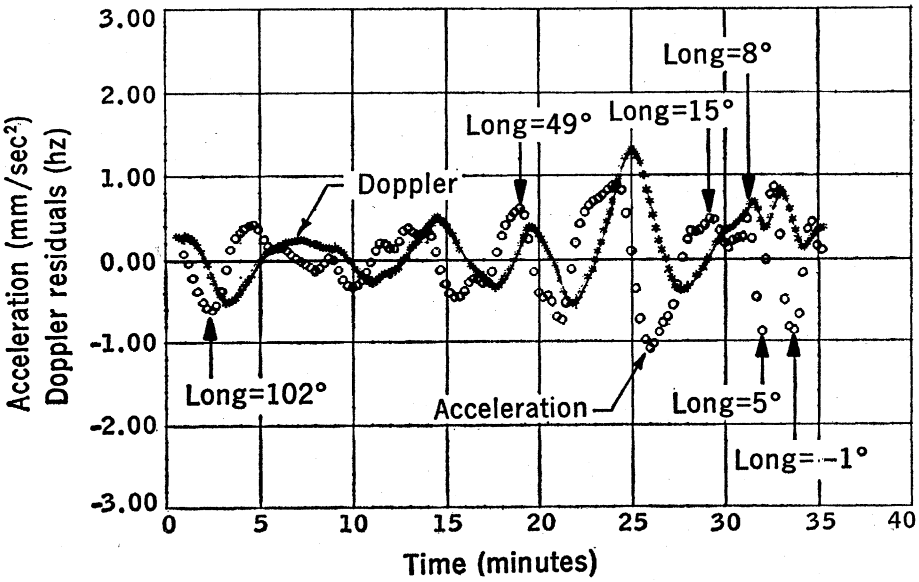

Fig. 3. Earthward velocity residuals (asterisks), and resulting accelerations (circles), after an orbit determination made by means of the 20th degree and order model.

The residual accelerations common to both Figs. 1 and 3 provide the following information on the lunar gravity fine structure:

1) The pair of sharp negative accelerations at longitude 5° and longitude −1° strongly imply negative mass anomalies at the craters Albategnius and Ptolemaeus, respectively. If lines are drawn through these points of peak negative acceleration, in a direction perpendicular to the trajectory ground trace, the lines pass through the centers of these craters as shown in Fig. 2. The actual peak residual accelerations, remaining after fits with both triaxial and 20th degree and order gravity models, are summarized in Table 1 together with the corresponding spacecraft altitude and the estimated depth of the equivalent mass deficiency required to produce these negative accelerations. These negative mass estimations were based on the somewhat smaller residual accelerations remaining after the 20th order fit. The reduction in the largest residual (near Mare Nectaris and the trajectory ends) provided by the 20th degree model suggests that this model produces the more believable fine structure gravity.

2) The negative peak acceleration at longitude +102° suggests a mass defect associated with the unnamed crater at latitude −12°, longitude 105° (the longitudinal position is shifted to restore the distortion caused by viewing geometry near the limb). The parameters of this feature are given in Table 1. We must, however, admit that the small residual accelerations remaining after the 20th degree and order fit could indicate that much of the apparent acceleration is due to the least-squares filter distortion of the effect of nearby Mare Smythii.

3) The two positive acceleration peaks at longitudes 7° and 2° are probably due to the highland ridges near craters Albategnius and Ptolemaeus.

4) The broad positive acceleration peak at longitude 48° (altitude, 38 km) may be due to a filled region of Mare Fecunditatis. Although this feature is broad enough to be resolved at Lunar Orbiter altitudes (100 km), it would be too small to show up strongly.

All the craters discussed here have negative mass anomalies (deficiencies). This is consistent with their formation by meteorite impact, with subsequent vaporization and ejection of large amounts of lunar and meteoritic material, or with any other mechanism that transports material out of a crater. This further indicates that only partial isostatic compensation has occurred. The highland ridges produce local relative, positive accelerations at these low altitudes. (These features had been lost in the broad negative background observed previously at higher altitudes.) The best example is the +20-mgal "ridge" at +15° longitude. This correlates closely with throwout shown on the preliminary lunar geological map of the U.S. Geological Survey. A low-altitude (25 to 50 km) subsatellite with S-band transponder would permit one to map large portions of the lunar surface to a resolution which is capable of producing geophysically significant information and correlations with other lunar data.

P. GOTTLIEB, P. M. MULLER
W. L. SJOGREN
Jet Propulsion Laboratory, California Institute of Technology, Pasadena
W. R. WOLLENHAUPT
National Aeronautics and Space Administration Manned Spacecraft Center, Houston, Texas 77058

References and Notes

1. P. M. Muller and W. L. Sjogren, *Science* **161**, 680 (1968).
2. P. Gottlieb, P. M. Muller, W. L. Sjogren, *ibid.* **166**, 1145 (1969).
3. P. Gottlieb, *Radio Sci.*, in press.
4. ——— and W. L. Sjogren, *Jet Propulsion Lab. Space Programs Sum. 37–60* (1969).
5. P. Gottlieb, *Jet Propulsion Lab. Space Programs Sum. 37–55* (1969), vol. 3, p. 3.
6. We thank L. Ross and R. Wimberly for the orbit determination and curve-fitting computations and A. O. Kiesow for the initial data processing. This report presents the results of one phase of research carried out at the Jet Propulsion Laboratory, California Institute of Technology, under NASA contract No. NAS 7-100.

29 December 1969

"Polywater": Possibility of p-Electron Delocalization

Abstract. p-*Electron delocalization may be important in determining the stability of the symmetric hydrogen bonds in a recently proposed model of "polywater."*

Lippincott *et al.* (*1*) have suggested a model for "polywater" in which symmetrical hydrogen bonds (O...H...O) are the basic components for constructing planar networks of hexagonal units. This model was criticized by Donohue (*2*) on the basis that eight different forms of ice and numerous hydrates have an angle between adjacent hydrogen bonds very near the tetrahedral angle, and hence that the 120° angles proposed by Lippincott *et al.* are unsatisfactory. However, similar reasoning, based on the observation of many thousands of aliphatic hydrocarbons, would lead one to conclude that ethylene is an unlikely species.

Table 1. Calculated stabilization energy and bond order.

Calculation	Energy stabilization, $O \cdots H \cdots O$ bond unit (kcal/mole)	Bond order, $O \cdots H$
1	16.1	0.60
2	118.9	0.78

The symmetrical hydrogen bonds were postulated (*1*) on the basis of infrared spectra of "polywater" and by analogy to the bifluoride ion. In the case of the bifluoride ion (FHF^-) a theoretical study and calculation by McLean and his co-workers (*3*) show that delocalization of the "lone-pair" *p*-electrons on the fluorine atoms takes place. This suggests that π-bonding is partially responsible for the unusual stability of the bifluoride hydrogen bonds.

This same sort of *p*-electron delocalization is possible in the model of polywater proposed by Lippincott *et al.* (*1*). The delocalization of the *p*-electrons on oxygen can be thought of as being transmitted by a hydrogen atom between any two oxygen atoms. This requires that the hydrogen atoms have some *p*-character. In the calculations for FHF^- hydrogen was indeed found to have such *p*-character (*3*).

The model, consisting of planar networks of hexagonal units (*1*), seems to be an ideal circumstance for the delocalization of the p_z electrons on the oxygens throughout the network to form a p-π band. This is analogous to what occurs in graphite, except that the bandwidth and occupation of the band would be different. On the basis of this model the electronic conductivity of "polywater" is expected to be significantly larger than that for normal water. Unfortunately, no conductivity measurements on "polywater" have been reported to date.

The prior theoretical calculations on "polywater" have been of the CNDO/2 (*4*) and INDO (*5*) types of semiempirical calculations, proposed by Pople and his co-workers (*6*), and have not made it possible to detemine whether the *p*-character of the hydrogens is important.

In the work reported here very approximate assessment was obtained of the importance of *p*-character in the hydrogen bonds. Calculations of the CNDO/2 type were modified to allow specifically for *p*-character in the hydrogens (*7*). The calculations for the $(H_2O)_6$ hexagonal unit are summarized in Table 1. In calculation 1 the O .... O distance was taken as 2.3 Å with the internal hydrogens placed symmetrically between the oxygen atoms. For a symmetrical hydrogen bond a distance between the two oxygen atoms of 2.3 Å gives a minimum in the energy. The external hydrogens were placed at 0.96 Å from the oxygen (the experimentally observed O–H distance in normal H_2O). All angles were taken to be 120°. Calculation 1 was a normal CNDO/2 calculation. Calculation 2 was identical to calculation 1 except that an extra basis function (a p_z orbital) was centered on the hydrogen atoms involved in hydrogen bonds.

Calculation 2 (Table 1) leads to a very large increase in stabilization. This large increase could be very much in error, however, because the basis set on hydrogen has been increased (by the addition of a p_z orbital) whereas the set of orbitals on the oxygens has been kept fixed. This procedure leads to an unbalanced basis set which can lead to an overestimation of the charge density in the vicinity of the hydrogen atom. Since the CNDO/2 method with the use of extended basis sets has not been calibrated against *ab initio* calculations in any published studies, it is difficult to estimate the error involved in the procedure used here. Although the numerical values obtained are certainly not quantitatively correct, the qualitative feature that *p*-electron delocalization can have a stabilizing effect could indeed be correct.

The stabilization energy is calculated by taking one-sixth of the difference between the binding energy of the $(H_2O)_6$ unit and six times the quantity (the binding energy of the H_2O unit, with no p_z orbitals on the hydrogens, at the experimentally determined geometry of an isolated H_2O).

The results presented in Table 1 may be compared with the estimates of Lippincott *et al.* (*1*) of a stabilization energy of 60 to 100 kcal/mole and a bond order of ⅔. The effect of *p*-electron delocalization also explains the recently